RMetS
Royal Meteorological Society

Economic impact of considering El Niño-Southern Oscillation on the representation of streamflow in an electric system simulator

Fernanda Maciel,[a] Rafael Terra[a]* and Ruben Chaer[b]

[a] *Instituto de Mecánica de los Fluidos e Ingeniería Ambiental, Facultad de Ingeniería, Universidad de la República, Montevideo, Uruguay*
[b] *Instituto de Ingeniería Eléctrica, Facultad de Ingeniería, Universidad de la República, Montevideo, Uruguay*

ABSTRACT: The Electric Power System Simulator (SimSEE) is a model that optimizes and simulates the operation of an electric system and has been widely used to analyze the integrated power system in Uruguay. Among the stochastic processes that SimSEE needs to represent are the streamflow inputs to the hydroelectric dams, which constitute a key factor for both energy dispatches and mid-term planning. A dominant feature of streamflow time series is that they show very high interannual variability, which represents a major uncertainty for energy operation in Uruguay. Part of this variability is associated with El Niño-Southern Oscillation (ENSO) phenomena. In this work, a climate index associated with ENSO is incorporated to the stochastic generator of streamflow series used by the SimSEE. Forty six-month-long simulations are performed with and without such modifications. We find that the system operator can take advantage of the ENSO-related information incorporated to SinSEE in 65% of the cases (semesters) considered, reducing the total costs of operation. This result still holds in a scenario with larger firm capacity. The amounts saved, however, are reduced as the firm capacity increases. The enhanced generation options associated with a larger firm capacity diminish the overall costs of generation, especially in times of low streamflow, rendering the savings associated with a more efficient management of the reservoir less significant.

KEY WORDS economic impact; electric system simulator; ENSO, stochastic process; streamflow representation

Received 9 November 2013; Revised 16 December 2014; Accepted 7 January 2015

1. Introduction

The Electric Power System Simulator (SimSEE; website: http://iie.fing.edu.uy/simsee), developed by Chaer (2008), is a model that optimizes and simulates the operation of an electric system and has been widely used to analyze short-term dispatch and long-term planning of the integrated power system in Uruguay (Chaer, 2009; Chipp *et al.*, 2012; Briglia *et al.*, 2013). SimSEE finds, through stochastic dynamic optimization, an operation policy (OP) that minimizes the expected value of the cost of future operation or Future Cost (FC), while the simulations allow us to compute the detailed operation of multiple realizations of the involved stochastic processes over the analyzed time horizon using the optimal OP.

SimSEE needs to represent those stochastic processes that characterize the uncertainty faced by the system. One of these processes is the streamflow input to the hydroelectric dams in Uruguay, which is a key factor for both energy dispatches and mid-term planning of the electric system, as hydroelectric generation represents typically more than 50% of the total generation (UTE, 2004-2012a). Currently, streamflow is characterized in SimSEE by a stochastic generator CEGH (Spanish acronym for 'Correlation in Gaussian Space with Histogram') at both the optimization and simulation stages (Chaer, 2005). CEGH generates synthetic time series with a linear autoregressive model in Gaussian space and transforms back into streamflow values using the nonlinear function that match the recorded streamflow histograms (one per week).

A dominant feature of streamflow time series is that they show very high interannual variability, which represents a major uncertainty for energy planning in Uruguay (León *et al.*, 2011). Part of this variability, according to Mechoso and Pérez-Iribarren (1992), is associated with El Niño-Southern Oscillation (ENSO, Aceituno, 1992) phenomena. ENSO influence, whose magnitude and lead time present a marked seasonality (Cazes-Boezio *et al.*, 2003), is not currently considered in streamflow modelling within the standard CEGH/SimSEE and is, therefore, not well represented (Maciel *et al.*, 2012).

The incorporation of climate information related to ENSO in CEGH/SimSEE was first studied by Chaer *et al.* (2010). They used a different methodology to the one presented here, simply limiting the historical streamflow record used for calibrating CEGH to those – analog – years in which ENSO was in a similar state, by some criteria, to the situation of interest. The study is limited to 1 year, August 2009 to July 2010, when an El Niño event was developing. They found that considering

* Correspondence to: R. Terra, IMFIA – Facultad de Ingeniería – Universidad de la República, Julio Herrera y Reissig 565, Montevideo, 11300, Uruguay. E-mail: rterra@fing.edu.uy

information related to ENSO allowed for a 10% reduction in the expected operation costs for the particular period analyzed.

A procedure to incorporate information of ENSO in CEGH, similar to the one described in Section 3, was developed by Maciel *et al.* (2012), who further tested its impact in the statistical properties of synthetic time series. They concluded that long-term statistics of simulated streamflow are highly improved, together with their mid-term (seasonal) predictability. Particularly, a better performance is noted during droughts, when operating costs increase. However, they could not evaluate the effect on the OP and the associated economic impact, since the new version of CEGH was not implemented in SimSEE.

In this work, a climate index associated with ENSO is incorporated to the stochastic generator of streamflow series CEGH and, in turn, to SimSEE. Forty six-month runs are performed with and without considering information related to ENSO. We thus evaluate the effect of this climatic information in the seasonal energy planning and estimate resource savings. Since ENSO influences climate in several regions in the world, the procedure here presented and evaluated could help introduce ENSO signal to decision-making processes in the energy sector elsewhere.

In Section 2, we present the data used in this study. Section 3 describes the methodology that defines the climatic predictor related to ENSO and describes how to incorporate it into the streamflow generator. Section 3.5 presents the two scenarios of the electric power system used. Results are presented in Section 4 and main conclusions in Section 5.

2. Data

We used weekly historical time series of streamflow in the three main hydroelectric dams of Uruguay: Rincón del Bonete, Salto Grande and Palmar (Figure 1), between 1909 and 2009. This information was provided by the national electric utility UTE (www.ute.com.uy). The remaining hydroelectric power plant, Baygorria, is immediately downstream Rincón del Bonete and has virtually no reservoir of its own, so its installed capacity is conflated with that of Rincón del Bonete.

On the basis of this data, we can compute an energy-weighted average, obtaining a weekly time series named complexive streamflow, as specified by Equation (1).

$$\text{Complexity Streamflow} = \frac{115 \times S + 618 \times B + 277 \times P}{115 + 618 + 277} \quad (1)$$

where S, B and P are streamflow to Salto Grande, Rincón del Bonete and Palmar dams, respectively. The coefficients are the capacity of the plants per unit of mean streamflow (in MW m^{-3} s^{-1}). The complexive streamflow is currently used in the operation of the system by the national electric utility (UTE) to reduce the number of state variables of the system for the Stochastic Dynamic Programming algorithm during the optimization phase that renders the OP (see Section 3.3).

Figure 1. Location of the three main hydroelectric dams of Uruguay.

Both the energy demand (with an annual total of 13,340 GWh) and the capacity of the electric power system used in the simulations represent a simplified version of the expected scenario for the near future. This simplified scenario is based on the current energy scenario (UTE, 2012) and an optimum expansion plan of the electricity generation (León *et al.*, 2011). The system capacity consists of 1140 MW of thermal power and 1541 MW of hydroelectric power which corresponds to Bonete (including Baygorria), Palmar and the Uruguayan fraction of Salto Grande plants.

Of the thermal power, 200 MW are gasoil powered turbines, with a cost of 200 USD MWh^{-1}, 920 MW are natural gas and fuel oil powered generators, with a cost of approximately 110 USD MWh^{-1}, and 20 MW are biomass generation, with a cost of 50 USD MWh^{-1}.

To represent the climatic information associated with ENSO, we use the monthly index Niño 3.4 (N3.4, Trenberth, 1997) between 1908 and 2009. This data, that represents the average sea surface temperature over a region in the central equatorial Pacific Ocean, is available at www.cpc.ncep.noaa.gov/data/indices/sstoi.indices.

3. Methodology

3.1. Climatic predictor

It is well documented that the influence of ENSO on the regional climate (in particular, precipitation and streamflow) varies through the year (Ropelewski and Halpert, 1987; Mechoso and Pérez-Iribarren, 1992; Pisciottano *et al.*, 1994; Cazes-Boezio *et al.*, 2003). Therefore, we assess, for each weak of the year, the optimal lead time at which N3.4 has maximum predictability on streamflow, for which we devised two alternative methods:

- Maximum correlation between the complexive streamflow series for each week and N3.4 monthly index with some lead time.

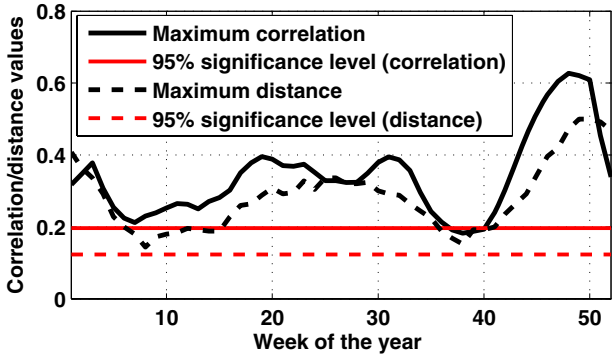

Figure 2. Annual cycles of: maximum correlation between streamflow and N3.4 (solid line) and maximum distance between streamflow distributions conditioned to N3.4 (dashed line). In both cases N3.4 has a certain (optimal) lead time *versus* streamflow. 95% confidence levels are plotted with the respective line type.

- Maximum distance between cumulative distributions of complexive streamflow conditioned by N3.4 monthly index with some lead time. For each week of the year, 50% of 'coldest' years (lowest values of N3.4) are compared with 50% of 'warmest' years, according to the N3.4 index with leads running from 0 to 12 months. The lead time that maximizes the distance between conditioned distributions is then found for each week of the year.

Figure 2 shows the annual cycle of maximum correlation between N3.4 with a certain lead time *versus* streamflow, and maximum distance between streamflow distributions conditioned to N3.4 with its own – potentially different – optimal lead time. Also shown are the 95% significance confidence levels that reject the null hypothesis that the variables are not correlated or the distributions are the same (following Kolmogorov–Smirnov test), respectively. While the seasonality of ENSO influence on streamflow is evident, it shows that there is indeed a significant signal throughout most of the year.

Next, Figure 3 shows the optimum lead time computed with both methodologies, which generate very similar results. This result is important because, as will be shown in the next section, the influence of ENSO on streamflow is incorporated after normalization of the time series, a process that does not conserve correlations but does conserve the other statistics. Lead times are also very similar (not shown) if we consider the streamflow of each individual hydroelectric dam instead of the complexive streamflow. An intermediate and smoothed lead time is produced (see Figure 3) and used hereafter. Finally, a weekly time series of the predictor index is constructed taking, for each week of the year, the value of N3.4 associated to the optimum lead; we call this series N3.4-OL.

3.2. Incorporation of N3.4-OL to the streamflow generator

SimSEE uses CEGH model as a generator of streamflow and other stochastic variables. CEGH first constructs nonlinear functions, and their inverse, to transform weekly

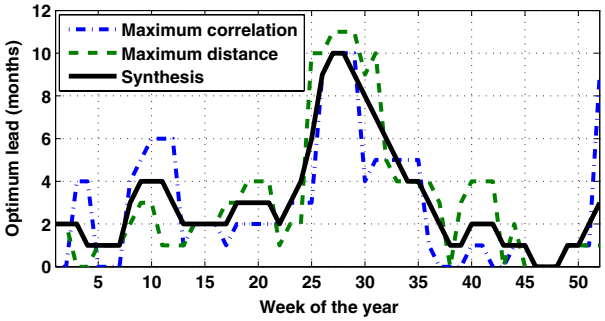

Figure 3. Optimum lead time of N3.4 index computed with two methodologies: maximum correlation (dotted line) and maximum distance (dashed line); see text for details. An intermediate smoothed version is plotted with a solid line.

histograms of historical streamflow series (real space) into normal distributions (Gaussian space). This histogram or quantile matching technique is selected for convenience and in no way imply that the streamflow distributions are normal, which they are not. The convenience of working in Gaussian space comes from the fact that the linear combination of independent normally distributed variables is also normal, which simplifies the modelling that is introduced next. A first order autoregressive model is calibrated and used to generate streamflow synthetic series in Gaussian space, as shown in Equation (2).

$$\begin{bmatrix} B \\ P \\ S \end{bmatrix}_{k+1} = [C\,(3\times 3)] \times \begin{bmatrix} B \\ P \\ S \end{bmatrix}_{k} + [A\,(3\times 3)] \times w_k\,(3,1)$$
$$= \begin{bmatrix} 0.678 & 0.083 & 0.118 \\ 0.087 & 0.672 & 0.030 \\ 0.040 & 0.010 & 0.815 \end{bmatrix} \times \begin{bmatrix} B \\ P \\ S \end{bmatrix}_{k} + A \times w_k \quad (2)$$

Streamflow to Rincón del Bonete (B), Palmar (P) and Salto Grande (S) dams during the $(k+1)$th week is computed multiplying streamflow of the kth week by matrix C, which captures the auto and cross-correlations with a lag of 1 week plus correlated Gaussian white noise $A \times w_k$. Matrix C is calibrated by least mean square using historical data. Once C is known, A is determined so that the covariance of synthetic time series coincides with the observed covariance (Chaer, 2013), thus capturing the simultaneous correlation of incremental streamflow in the neighbouring basins.

As the linear transformation of a Gaussian process is also Gaussian, the shape of streamflow series histograms is conserved once the inverse functions are applied and the synthetic time series in 'real space' are obtained. In addition, 1 week correlations and autocorrelations in Gaussian space are maintained by construction, while the correlations in real space are only approximately conserved.

The system in Equation (2) is the original system used by SimSEE and the base for the incorporation of ENSO influence. We call this system BPS, for it only considers streamflow information.

In Equation (3), N3.4-OL index is incorporated to the autoregressive system. We call this system BPSN, where

N represents N3.4-OL index. The coefficients of matrix $C_k(4 \times 4)$ are calibrated using weekly historical data of streamflow and N3.4-OL (1909–2009). Unlike BPS system, matrix C_k varies with the week of the year (1–52). This enables the system to capture the seasonality of the relation between N3.4-OL and streamflow.

$$\begin{bmatrix} B \\ P \\ S \\ N \end{bmatrix}_{k+1} = \left[C_k\,(4\times 4)\right] \times \begin{bmatrix} B \\ P \\ S \\ N \end{bmatrix}_{k} + \left[A_k\,(4\times 4)\right] \times w_k \quad (3)$$

Equation (3) could either be used in a 'free' mode, synthesizing all four variables, or prescribing the trajectory of any one of the variables, for instance N. In this way, we are able to generate many possible realizations of B, P and S, conditioned to a certain evolution of N, which is assumed to be known or subject of an independent prediction. Moreover, for simulation times shorter than the optimum lead time, future values of N3.4-OL have already been observed.

As we want to compare simulations with and without considering N3.4-OL, it is convenient to modify the BPS system in Equation (2) including a 'mute' variable 'x' that occupies the dimension of N but does not affect the simulation of B, P and S streamflow (as in Equation (4)), and consequently does not affect the OP; we call this system BPSx.

$$\begin{bmatrix} B \\ P \\ S \\ x \end{bmatrix}_{k+1} = \begin{bmatrix} 0.678 & 0.083 & 0.118 & 0 \\ 0.087 & 0.672 & 0.030 & 0 \\ 0.040 & 0.010 & 0.815 & 0 \\ 0 & 0 & 0 & 0.974 \end{bmatrix} \times \begin{bmatrix} B \\ P \\ S \\ x \end{bmatrix}_{k} + \left[A_k\,(4\times 4)\right] \times w_k \quad (4)$$

3.3. Optimization phase

The optimization phase determines the OP by minimizing the present value of expected future operation costs: generation costs plus costs associated to the failure in supplying the energy demand. The discretized version is:

$$\min \sum_{k=0}^{k=\infty} q^k \left[\left(\sum_{i=1}^{i=N} cv_{i,k} E_{i,k} \right) + cv_{f,k} E_{f,k} \right] \quad (5)$$

In Equation (5), k is the time step ordinal (weekly in our case), q is the discount rate, $cv_{i,k}$ and $E_{i,k}$ are the unit cost and energy dispatched by generator i, respectively, while $cv_{f,k}$ and $E_{f,k}$ are the unit cost of failure and the energy that could not be supplied; everything for time step k. The decision variables are $E_{i,k}$ and $E_{f,k}$ under the constraints of the energy demand and availability of generators at each time step.

In theory, the optimization period should be indefinitely extended in time (as in Equation (5)), as the future costs extends to an infinite time in the future. As the model includes a discount rate q for future costs, the present value of future costs tends to zero as time progresses. In this work, we extend the optimization period for at least 10 years after the end of the simulation period.

The unit production costs for each thermal generator and the cost of failure ($cv_{i,k}$ and $cv_{f,k}$) are known at each time step (the latter being fixed by the administration). The unit production costs of wind and hydro-based generators are zero. However, in the case of the hydroelectric plants, the present use of stocked water potentially increases future production costs, because the resource will no longer be available. Conversely, the preservation of water for later use may reduce future costs, but it increases the present direct costs (DC), due to the additional thermal generation that will be required.

To address the problem, SimSEE uses a stochastic dynamic programming algorithm (Bellman, 1957), which computes the future cost (FC) as a function of the state of the system and time. For each time step k and each state, the function gives the minimum expected cost of operation, from a given time step forward. In this work, the state of the system is associated with the volume of water in the reservoirs, the complexive streamflow in the previous time step and the climatic predictor. In dynamic programming, the optimization problem is solved for each time step backwards in time, starting from the last time step in which the solution is known because FC is considered zero at the end of the optimization period.

The FC function constitutes the OP of the system; it is used during the simulation phase to decide the dispatch of energy. Dispatch is determined by minimizing the sum of DC incurred at each time step plus FC at the end of the time step, which depends on the operation because it modifies the state of the system, for instance, the level of the reservoir. Accordingly, the water in the reservoirs is given a value that is minus the derivative of the FC with respect to the resource at the end of the time step. Thus, if the use of a certain volume of water at this time step implies savings in DC that are larger than the increase in the FC caused by the variation of the system state associated with the extraction of water, the decision will be to use that volume, and *vice versa*.

According to the role of N3.4-OL, four different types of optimizations can be carried out:

- BPSx: Aside from the presence of 'x', which has no consequence, this corresponds to the current standard CEGH, with no climatic information related to ENSO.
- BPSN-free: The historical relation between ENSO and streamflows is incorporated during calibration. Even though there is no information about the future evolution of N3.4-OL during the optimization phase, the much larger inertia of this variable (as reflected in C(4,4) in Equation (4)) will help spread the effect of the N3.4-OL initial condition in simulations with time horizons comparable to the time-scale of change of ENSO.
- BPSN-pred: Predictions of N3.4-OL are used during the optimization phase to impose the trajectory of N. Predictions of N3.4-OL are constructed using N3.4 historical predictions existing at the initial time of each optimization period in IRI (The International Research Institute

for Climate and Society), which are available at portal.iri.columbia.edu/portal/server.pt starting in 2002.
- BPSN-obs: The trajectory of N3.4-OL is prescribed during the optimization phase according to the observed evolution. It represents the scenario of a perfect ENSO prediction.

First, we perform a long optimization run from 2002 to 2020 (or rather from 2020 to 2002 since the optimization phase progresses backwards in time) with the BPSN-free system. It was verified that further extending the optimization period did not affect the OP for the dates of interest; differences in the present value of Future Costs beyond 2020 are negligible. The long optimization run gives the OP for the BPSN-free configuration, but not yet for the other configurations as no information regarding the future evolution of N3.4-OL is 'seen' by the OP. For other configurations, an additional 6-month optimization sub-period (performed with the respective systems) is concatenated to the future cost function of the longer run at the end of each semester that will later be simulated. This reduces computation time (as compared to making independent long optimizations for each system) and facilitates the comparison of the results obtained with the different systems, because they all see the exact same long-term future costs from the long optimization run.

The concatenation is straight forward for the BPSN-pred and BPSN-obs systems, because they copy the future cost function from the long run at the concatenation point, which depends on the level of Rincón del Bonete dam, the hydrologic condition (directly related to the complexity streamflow) and the value of N3.4-OL. (Palmar and Salto Grande dams do not store water for more than a week – the time step used – therefore Rincón del Bonete is the only dam with a reservoir.)

For the BPSx system, the future cost function depends on the level of Rincón del Bonete dam and the hydrologic condition only. Thus, the future costs are averaged in the N3.4-OL dimension at the concatenation point, since the condition of N3.4-OL is represented by quintiles with equal probability. The existence of an x variable that is 'mute' but analogous to N facilitates the instrumentation of this step.

3.4. Simulation phase

A set of 40 six-month-long overlapping simulations, starting on the 1st day of February, May, August and November from 2002 to 2011, respectively, were performed for each type of system (BPSx, BPSN-free, BPSN-pred and BPSN-obs). The period was chosen because there are both N3.4 predictions (except for February 2002) and observations available. The simulation period coincides with the optimization sub-period, in which is concatenated to the much longer main optimization run that extends 10 more years at the least.

Simulations are performed following the observed streamflow to the hydroelectric dams throughout the semester, so that the real (observed) trajectories of B, P and S are prescribed. Thus, we can compute the impact of the different optimization strategies on what really happened. Statistical significance is obtained through the combined analysis of all 40 semesters. Still, 100 simulations are performed for each semester, differing in the other stochastic variables: wind speed that affects wind power generation and the lucks that determine whether generators are available or broken.

3.5. Scenarios of the electric power system

To better evaluate the effect of incorporating N3.4-OL to the system we restrict other possible sources of variability that could hinder the interpretation of the results. Therefore, the annual electricity demand and the prices of fuels are kept constant during both optimization and simulation phases.

However, there is one aspect of the energy system to which we want to analyze the sensitivity of the results, namely, the effective firm capacity defined as the power that is reliably available to supply the electricity demand at all times. For thermal power plants, it is calculated multiplying the nominal power by the measured availability factor of each generator. In the case of hydroelectric plants it depends on the hydrology and the capacity of the reservoirs. It is here defined as the average monthly power that the hydroelectric system is capable of delivering with a probability of 95% based on the historical record. In the case of wind generation, the instantaneous firm power is zero due to intermittency. However, the firm energy during a longer period of time, say a week, is larger than zero. Moreover, the combination of hydroelectric generation (that can be dispatched in demand but has limited firm energy for extended periods due to climate variability) and wind generation (that has zero firm power but has a finite reliable energy output for long periods of time) generates effective firm capacity in the system. Such is the logic for the planned expansion of the Uruguayan electric system, because the hydraulic system is able to filter weekly variations in wind generation up to at least 1200 MW of distributed wind power (Chaer *et al.*, 2012). In this way, the incorporation of distributed wind generation will increase the weekly firm energy of the system as a whole, the one you can expect to have with a probability of 95%. A detailed description of how wind generation is included in SimSEE can be found in Cornalino *et al.* (2010).

Currently, the level of firm capacity is relatively low. Consequently, the dispatch of the hydroelectric plants is quite conservative since it risks failure. As the system improves in this respect, the hydroelectric plants can be dispatched more aggressively and, potentially, this could change the economic impact of incorporating climatic information in the decision.

The Uruguayan electric system is rapidly incorporating wind generation. For this reason we construct two scenarios in which to compute the economic impact of incorporating ENSO information in SimSEE.

- 400 MW of wind energy which will be met by the end of 2014.

- 1200 MW of wind energy, planned expansion for the next few years.

Both scenarios have a constant annual demand, hydroelectric and thermal power capacities as described in Section 2.

4. Results

4.1. Valorization of water at the beginning of the simulation period as a function of N3.4-OL for each scenario

During the optimization phase, SimSEE computes the value of water at Rincón del Bonete dam for each state of the system. Indeed, this value is precisely what determines the OP and enables the selection of the cheapest generator to dispatch at each time step during the simulation.

As, for each starting date, all simulations share the same initial state of the reservoir (the one observed at the time) and hydrologic state (associated with the recorded complexive streamflow the previous week), the initial value of water in the reservoir may only differ due to different expectations of future streamflow inputs associated with different optimization strategies. We next compare, for each starting date, the difference of the value of water at Rincón del Bonete dam (in dollars per cubic hectometre of water) between configurations BPSx and BPSN-free and associate the difference with the anomaly of N3.4-OL at the time. Figure 4 shows such relation for the scenario with low firm power capacity.

The difference in initial value of water (BPSN minus BPSx) is negatively correlated with N3.4-OL anomalies. In other words, when N3.4-OL has a positive anomaly, on average BPSN-free system valorizes the water less than BPSx. This is expected considering that, as was stated in the introduction, positive/negative values of N3.4-OL are associated – in certain seasons – with increased/decreased precipitation in the region.

The correlation is not perfect since the value of water is greatly affected by the level in the reservoir (not shown in Figure 4). In addition, as has been stated already, the influence of ENSO on streamflow varies through the year, which is reflected for instance in the smaller amplitude of ENSO signal – difference of initial value of water – for August 1st, a time that phases a period of low predictability (see Figure 2).

4.2. Evaluation of future costs at the end of the simulation period

To evaluate the economic impact, we need to compare total costs (TC) for each situation, adding the direct costs (DC) incurred during the simulation plus the future costs (FC) at the end of the semester. Differences in FC at the end of the simulations arise from different operation of the hydroelectric plants during the semester and are reflected in the level at Rincón del Bonete. Other states of the system are identical in all cases: N3.4-OL (if considered at all) does not depend on the operation and the hydrological state

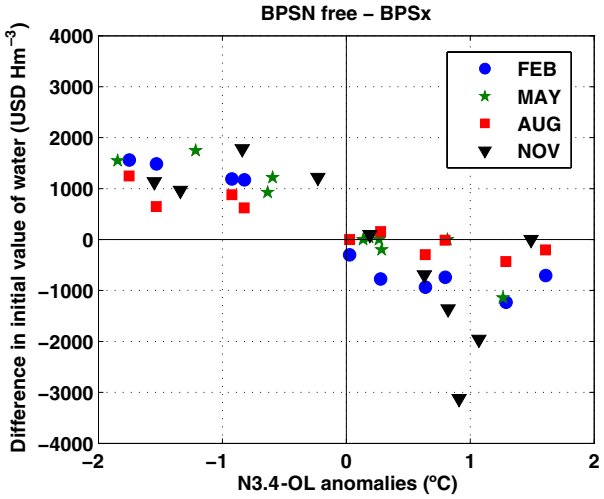

Figure 4. Scatter plot of N3.4-OL anomalies and difference in value of water between systems BPSN-free minus BPSx at the beginning of each semester.

is also the same since we are simulating on the historical trajectory of streamflow time series.

The FC is obtained from the long term optimization run with BPSN-free at the end state of the simulation. This procedure can be used even in the BPSx case that does not consider N3.4-OL.

4.3. Results for the first energy scenario

We first average the 100 simulations performed for each semester and for each system and then compare BPSN-free with BPSx. Figure 5 plots the difference (BPSN-free minus BPSx) in accumulated DC (in millions of dollars) during the 6-months-long simulations against the N3.4-OL anomaly at each starting date. Negative (positive) values in Figure 5 represent a reduction (increase) in direct costs associated to the different OP. In general, when N3.4-OL has a positive (negative) anomaly BPSN-free expects a wetter (drier) season and therefore takes more (less) risks, incurring in less (more) direct costs.

However, it is also true that an OP that is more (less) aggressive in the use of hydropower generators will leave a lower (higher) level in the reservoir at the end of the period, as can be verified in Figure 6. In turn, this will reflect in higher (lower) FC that will tend to balance the lower (higher) DC. Note that the simulations are performed over the observed realizations of streamflow, therefore the differences in reservoir level at the final time can only be attributed to differences in operation.

What ultimately matters are the total costs (TC = DC + FC), which consider both the savings – or overcosts – during the semester and the valorization of the water in the reservoir at the end of each simulation period. Figure 7 shows the differences in TC between BPSN-free and BPSx, where negative values represent net savings that can be attributed to the incorporation of N3.4-OL to the system (and positive values represent overcosts). Indeed, BPSN-free has lower TC in most cases (65% of

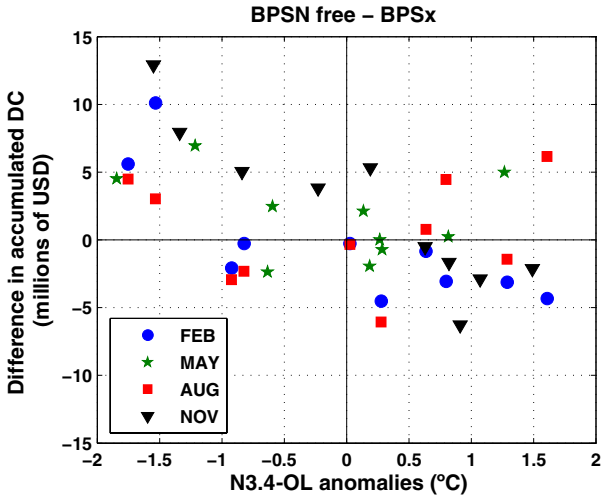

Figure 5. Scatter plot of the difference in accumulated DC between systems BPSN-free and BPSx during each semester-long simulation against N3.4-OL anomaly at the starting date.

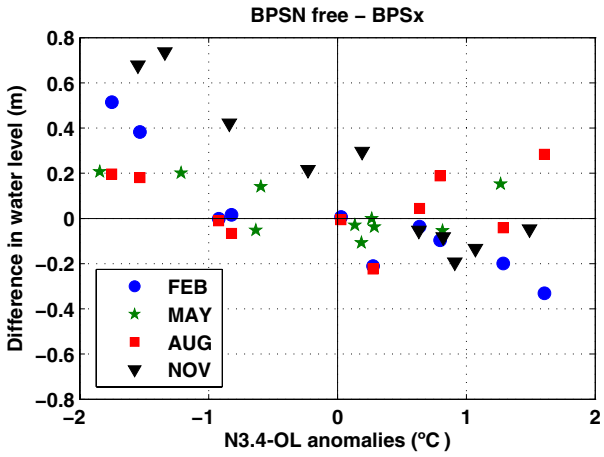

Figure 6. Scatter plot of the difference in water level at Rincón del Bonete dam between systems BPSN-free and BPSx at the end of each semester-long simulation against N3.4-OL anomaly at the starting date.

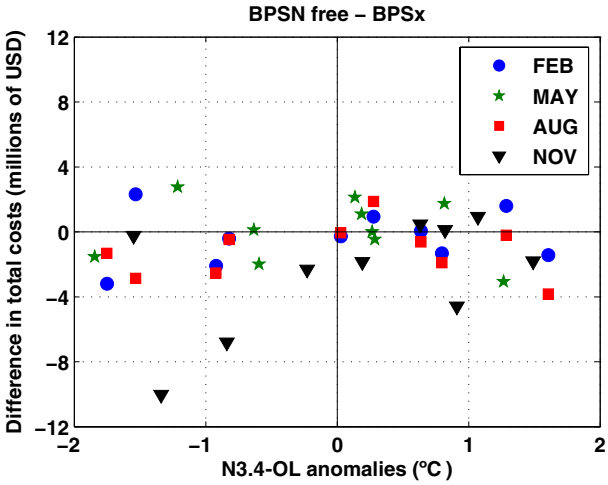

Figure 7. Scatter plot of the difference in TC between systems BPSN-free and BPSx against N3.4-OL anomaly at the starting date.

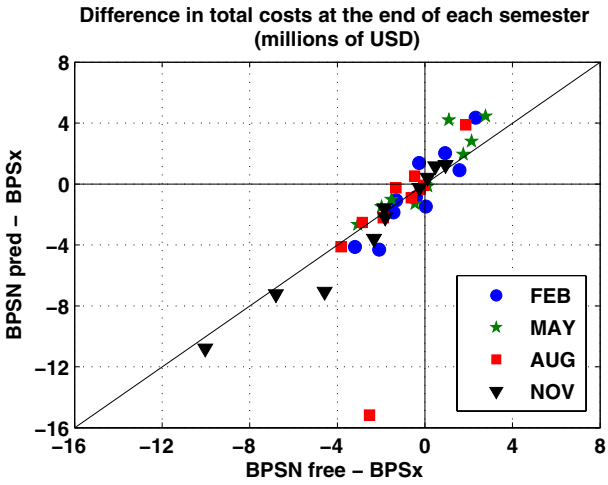

Figure 8. Scatter plot of the difference in TC between systems BPSN-pred and BPSx against the difference between systems BPSN-free and BPSx.

the time). Savings can be as high as 10 million dollars while loses are not larger than 3 million.

BPSN-free performance is clearly better when N3.4-OL anomalies are negative, which coincide with the more costly years due to a larger share of thermal generation. The semester starting in August presents the best results in general, while the one starting in November presents the best results when N3.4-OL anomalies are negative. Semesters starting in May or February present mixed results, on average they do not generate savings or loses over the several years.

Finally, we evaluate whether an additional benefit is obtained when N3.4-OL trajectories are imposed during the optimization stage by using either predicted (BPSN-pred) or observed (BPSN-obs) data. Figures 8 and 99 show the effect in TC of imposing the trajectory of N3.4-OL during the optimization phase, with predicted and observed data, respectively, as compared to the results obtained for BPSN-free. Except for a particular case in August, we conclude that prescribing N3.4-OL trajectory during the optimization phase does not have significant additional benefits.

4.4. Results for the second energy scenario

The implications of changing the energy scenario to one with larger firm capacity can first be detected through its effect on the valuation of water, which directly affects the OP. Figure 10 compares the differences in initial value of water (BPSN-free minus BPSx) for both energy scenarios.

The results in Figure 10 tend to be aligned along the main diagonal, which shows that they are very similar in both energy scenarios. It is also evident that the inclusion of N3.4-OL in the system has the greatest impact in the valuation of water for the semesters starting in November and February and the least impact in August. However, the magnitude of the differences in the initial value of water is smaller for the second energy scenario, especially

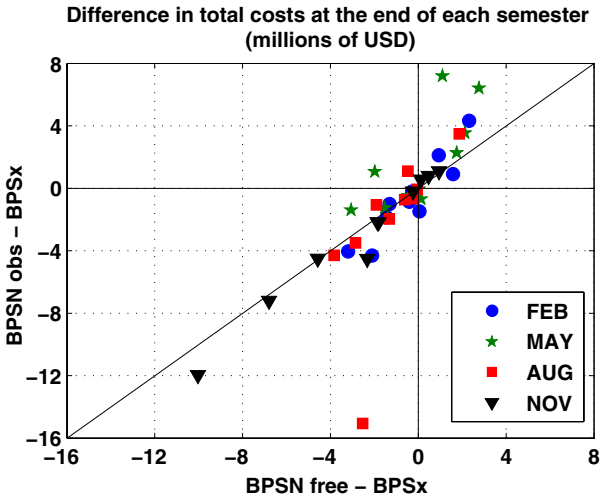

Figure 9. Scatter plot of the difference in TC between systems BPSN-obs and BPSx against the difference between systems BPSN-free and BPSx.

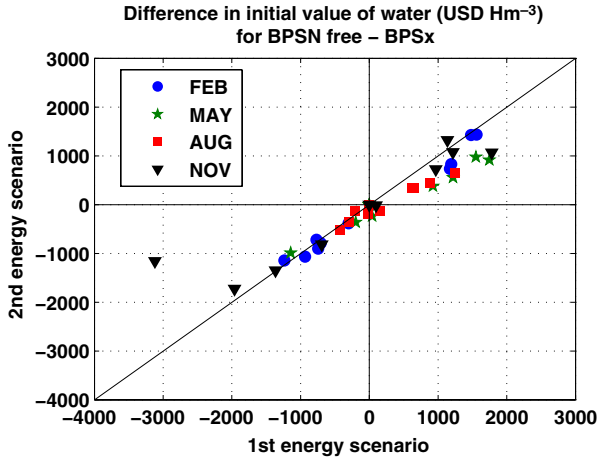

Figure 10. Scatter plot of difference in initial value of water between systems BPSN-free and BPSx for both energy scenarios.

for positive values of the difference, when BPSN-free expects a dry season (N3.4-OL values are negative as shown in Figure 4). This is coherent with the fact that the larger firm capacity reduces the costs, especially in periods of low hydroelectric generation. With lower firm capacity, the system has to resort to the most costly options (including failure to cover demand) when facing a period of low streamflow. In such situations, the ability to alert of an upcoming drought – which are in part related to ENSO – allow for better management of the reservoir and can result in significant savings. As the firm capacity becomes larger, this effect is less prominent in the results because the system has more generation resources to totally or partially avoid failure.

In addition, Figure 11 compares the differences in the TC (BPSN-free – BPSx) for both energy scenarios and shows that in most cases BPSN-free has lower cost than BPSx (67.5% of the time) regardless of the firm power capacity of the system. Deviations from the main diagonal

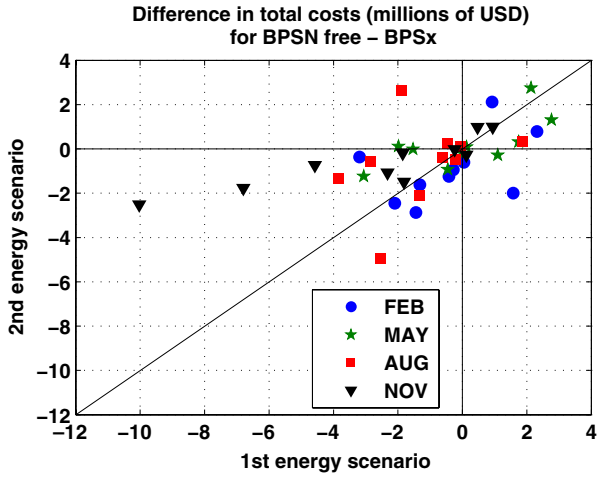

Figure 11. Scatter plot of difference in TC between systems BPSN-free and BPSx both energy scenarios.

are most evident in the simulations that show the highest savings for the first energy scenario (they are significantly reduced in the second), corresponding to semesters starting in November.

5. Conclusions

The incorporation of information related to ENSO into SimSEE through N3.4-OA index improves the performance of the electric power system planning in a seasonal time scale. These improvements are measured through the Total Costs at the end of each semester, a result that encourages the development of similar approaches in other regions affected by ENSO.

Approximately two-thirds of the cases (semesters) show net savings due to the implementation proposed, a result that is independent from the system firm capacity. However, the amounts saved are reduced as the firm capacity increases. The system with low firm capacity is more vulnerable to variations in hydropower generation. By increasing its firm capacity, the generation options are enhanced, diminishing the overall costs of operation, especially in times of low hydroelectric generation. Therefore, the savings associated to a more efficient management of the hydroelectric reservoir (considering ENSO information) decrease.

Finally, it is found that prescribing the N3.4-OA trajectory during the optimization (through BPSN-pred or BPSN-obs) does not seem to bring a significant additional benefit, confirming that the inertia of ENSO phenomenon during a semester is enough to capture the signal.

Acknowledgements

This work was supported by ANII (National Agency for Research and Innovation of Uruguay), project PR_FSE_2010_31.

References

Aceituno P. 1992. El Niño, the Southern Oscillation, and ENSO: confusing names for a complex ocean–atmosphere interaction. *Bull. Am. Meteorol. Soc.* **73**: 483–485.

Bellman R. 1957. *Dynamic Programming*. Princeton University Press: Princeton, NJ. ISBN: 0-486-42809-5.

Briglia E, Ron F, Esponda P, Bouvier A, Alaggia S, Abreu N. 2013. Integración del Mercado Eléctrico y el mercado de gas natural en los modelos de optimización y simulación del SimSEE. In *4° Encuentro Latinoamericano de Economía de la Energía (ELAEE)*, Montevideo, Uruguay, 8–9 April.

Cazes-Boezio G, Robertson AW, Mechoso CR. 2003. Seasonal dependence of ENSO teleconnections over South America and relationships with precipitation in Uruguay. *J. Clim.* **16**: 1159–1176, doi: 10.1175/1520-0442(2003)16<1159:SDOETO>2.0.CO;2.

Chaer R. 2005. *Modelo de series correlacionadas CEGH*. Curso SimSEE, Instituto de Ingeniería Eléctrica, Facultad de Ingeniería, Universidad de la República, Montevideo. http://iie.fing.edu.uy/simsee/curso2010/Cap9_sintetizadorCEGH.pdf (accessed 10 February 2013).

Chaer R. 2008. *Simulación de sistemas de energía eléctrica*. Tesis de maestría en Ingeniería Eléctrica, Universidad de la República, Montevideo. http://iie.fing.edu.uy/publicaciones/2008/Cha08/Cha08.pdf (accessed 10 February 2013).

Chaer R. 2009. Simulación de granjas eólicas en el despacho óptimo del sistema hidro-térmico de generación de energía eléctrica del Uruguay. In *Anales del 2do Encuentro Latinamericano de Economía de la Energía (ELAEE)*, Santiago, Chile, 22–24 March, 1030–1047. ISBN: 978-956-14-1043-5.

Chaer R. 2013. Fundamentos del modelo CEGH de procesos estocásticos multivariables. Reporte técnico, Instituto de Ingeniería Eléctrica, Facultad de Ingeniería, Universidad de la República, Montevideo. http://iie.fing.edu.uy/simsee/biblioteca/CEGH_Fundamentos.pdf (accessed 16 April 2014).

Chaer R, Terra R, Díaz A, Zorrilla J. 2010. Considering the information of the Niño 3.4 index in the operation of the electrical system of Uruguay. In *Proceedings of the 33rd IAEE International Conference*, Rio de Janeiro, Brazil, 6–9 June.

Chaer R, Cornalino E, Coppes E. 2012. Modeling and simulation of the power energy system of Uruguay in 2015 with high penetration of wind energy. In *XII SEPOPE*, Rio de Janeiro, Brazil, 20–23 May, SP082 pp. http://iie.fing.edu.uy/publicaciones/2012/CCC12/CCC12.pdf (accessed 3 November 2014).

Chipp H, Prais M, Kligerman AS, Teles de Azevedo MH, Lattari LA, Casaravilla G, Chaer R, Cabrera J, Casulo A. 2012. Estabelecimento das condições para determinação dos benefícios da integração elétrica entre o Brasil e o Uruguai. In *XII Simpósio de Especialistas em Planejamento da Operação e Expansão Elétrica*, Rio de Janeiro, Brazil, 20–23 May. http://iie.fing.edu.uy/publicaciones/2012/CPKABCCCC12/ (accessed 3 November 2014).

Cornalino E, Chaer R, Ferreño O. 2010. Mejoras del modelado del recurso eólico de Uruguay en la plataforma SimSEE. In *EPIM'2010-IEEE*, Montevideo, 26–27 November. http://iie.fing.edu.uy/epim2010/myreview/myPapers/p77.pdf (accessed 3 November 2014).

León M, Castromán N, Larrosa D, Casaravilla G, Chaer R. 2011. Planificación de las inversiones de generación eléctrica con control de la volatilidad de los costos anuales de abastecimiento. In *3er Encuentro Latinoamericano de Economía de la Energía (ELAEE)*, Buenos Aires, Argentina, 18–19 April.

Maciel F, Terra R, Díaz A. 2012. Incorporación de información climática en la simulación de aportes a represas en un modelo del sistema eléctrico. In *Memorias del XXV Congreso Latinoamericano de Hidráulica*, San José, Costa Rica, 9–12 September. ISBN: 978-9968-933-06-3.

Mechoso CR, Pérez-Iribarren G. 1992. Streamflow in southeastern South America and the Southern Oscillation. *J. Clim.* **5**: 1535–1539, doi: 10.1175/1520-0442(1992)005<1535:SISSAA>2.0.CO;2.

Pisciottano G, Díaz A, Cazes G, Mechoso CR. 1994. El Niño-Southern Oscillation impact on rainfall in Uruguay. *J. Clim.* **7**: 1286–1302, doi: 10.1175/1520-0442(1994)007<1286:ENSOIO>2.0.CO;2.

Ropelewski CF, Halpert MS. 1987. Global and regional scale precipitation patterns associated with the El Nino/Southern Oscillation. *Mon. Weather Rev.* **115**: 1606–1626, doi: 10.1175/1520-0493(1987)115<1606:GARSPP>2.0.CO;2.

Trenberth KE. 1997. The definition of El Niño. *Bull. Am. Meteorol. Soc.* **78**: 2771–2777.

UTE. 2004-2012a. *UTE en Cifras – Año 2004 a 2012*. http://www.ute.com.uy/pags/Institucional/ute_en_cifras.html (accessed 10 February 2013).

UTE. 2012. *Memoria Anual 2012*. http://www.ute.com.uy/pags/institucional/documentos/memoria%202012%20para%20WEB.pdf (accessed 3 November 2014).